Transactions, **SMiRT-25**
Charlotte, NC, USA, August 4-9, 2019
Division XI

DISCUSSION ON FAILURE BEHAVIOUR OF PIPING SYSTEMS SUBJECTED TO EXCESSIVE SEISMIC LOADS

Izumi Nakamura[1] and Naoto Kasahara[2]

[1] Chief Researcher, National Research Institute for Earth Science and Disaster Resilience, Tsukuba, Ibaraki, Japan (izumi@bosai.go.jp)
[2] Professor, The University of Tokyo, Bunkyo, Tokyo, Japan

ABSTRACT

Experimental investigation on failure behaviours of piping systems were conducted with elbow pipes made of simulation materials to clarify the possible failure modes under the beyond design level seismic loads. The static loading test and shaking table test on a simple piping system model were conducted, and several failure modes were obtained. The most typical failure mode from the shaking table test was the ratchet and subsequent collapse. The configuration of piping system, input frequency, additional mass weight, input acceleration level were thought to be the factors to affect the failure modes. The experimental results indicated that it was crucial to understand the structure's ultimate behaviour when treating BDBE, and the investigation procedure using simulation materials was effective to investigate the ultimate behaviour of piping systems.

INTRODUCTION

As the lessons learned from Fukushima Dai-ichi Nuclear Power Plant (NPP) accident in 2011, the importance of consideration for Beyond Design Basis Event (BDBE) is widely recognized. In the design basis condition, it is required to realize the conservative design, and to include an enough margin to the actual strength of NPP's components to prevent any failure. In contrast to such conventional design approach, it is necessary to understand their ultimate behaviour and to take adequate countermeasures based on the rational strength estimation of the components under BDBE to prevent the fatal failure of structures (Kasahara and Sato (2017)).

Piping systems are one of the crucial components of NPPs, and it is thought to be the vulnerable components under the excessive seismic events. Plastic-collapse is the postulated failure mode under a seismic load in the conventional design rules, whereas the fatigue failure is the most probable failure mode from the various previous studies on piping systems made of steel even when the input acceleration was much higher than the design allowed level (Fujita et al. (1978), Tagart et al. (1990), Touboul et al. (1999), Yoshino et al. (2000), Nakamura et al. (2010), Varelis et al. (2013), Ravikiran et al. (2015)). Failure mode other than fatigue failure may occur under the extreme loading condition (Tagart et al. (1990)), although it is rare. It seems that much larger input acceleration and the extreme loading condition are necessary to conduct in-depth investigation of failure behaviours under BDBE. However, it is difficult to realize it in practice, due not only to the limitation of the performance of the testing facility but also to the safety concerns in conducting the experiment. Thus, the authors proposed a new experimental procedure using pipes made of simulation materials instead of steel pipes to investigate failure modes of piping systems under seismic loading (Nakamura and Kasahara (2015), Nakamura and Kasahara (2016), Nakamura and Kasahara (2018)). The simulation materials adopted in this experimental approach were pure lead (Pb) or lead-antimony (Pb-Sb) alloy. The strength of the simulation materials was much lower than that of the steel pipes, therefore the experiments under the extreme loading condition were enabled with the existing testing facilities. This paper introduces the experimental results of pipes made of simulation materials and discusses the possible failure modes of piping systems under excessive seismic load.

EXPERIMENTAL STUDY WITH PIPES MADE OF SIMULATION MATERIAL

Experiment with simulation materials

The experimental procedure of using simulation materials is based on the idea that failure modes of structures can be realized by the existing testing facilities if strength of the structures can be reduced (Nakamura and Kasahara (2015)). Figure 1 shows the stress–strain curves of Pb-Sb alloy including pure Pb in room temperature, and those of the carbon steel commonly used in the actual piping systems in several temperatures. Figure 1 depicts that the yield stresses of Pb-Sb alloys were less than 10% of that of the carbon steel. Moreover, the elastic-plastic behaviours of Pb-Sb alloys were analogous with that of the carbon steel. Such similarity of the stress-strain relationship indicated that the macroscopic plastic response behaviour of structures made of steel could be simulated by the structures made of Pb-Sb alloys. Figure 1 also shows that the material ductility of Pb-Sb alloy can be varied by controlling Sb ratio. Considering the difficulty of manufacturing pipes made of simulation materials, the composition ratio of Sb was set at 1% or 0% (pure Pb) in this study.

Static loading test

Static loading test on elbow pipes made of simulation materials was conducted to obtain the fundamental strength data. The simulation material used in the static loading test was Pb-Sb alloy. The target composition ratio of Sb was set at 1%. Table 1 shows the material property of Pb-Sb. Figure 2 shows the stress-strain curve of Pb-Sb. Straight pipes were manufactured by extrusion processing, and then, these pipes were bended to elbow shape. Figure 3 shows the configuration of the elbow pipe. Flanges were welded to the both ends of the elbow pipe so that the elbow pipe could be set on the testing machine. Figure 4 shows the experimental setup of the static loading test.

The loading conditions were monotonic in-plane bending in the direction to the elbow closing direction (compression), monotonic in-plane bending in the direction to the elbow opening direction (tension), and in-plane cyclic bending of the elbow opening and closing. The loading tests were conducted under the displacement-controlled condition, in room temperature, without internal pressure.

The monotonic loading tests were continued until the failure of the specimens or the limit of the test equipment. The amplitude of the cyclic loading tests was decided based on the result of the monotonic loading test so that the strain range at the elbow flank be approximately 2-10%. As a result, the loading amplitudes in the cyclic loading test were ±20 mm, ±40 mm, and ±65 mm. The cyclic loading tests were conducted until the failure of the specimens.

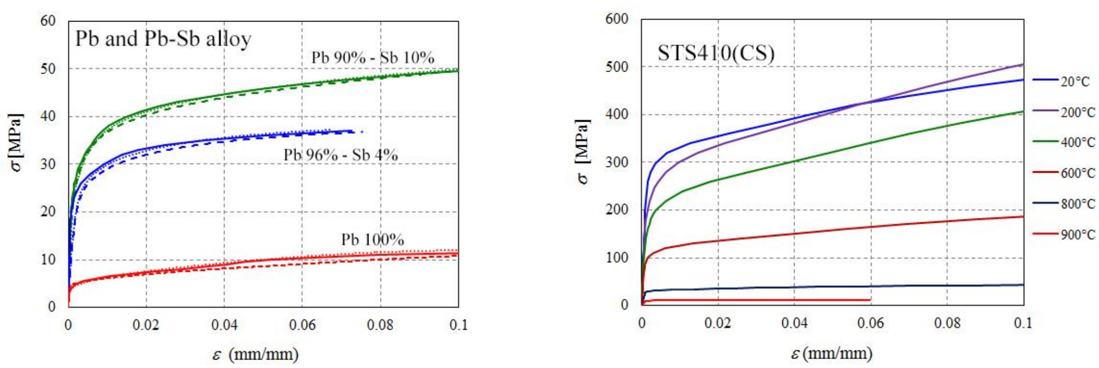

(a) Pb and Pb-Sb alloys (at 23°C) (b) Carbon Steel (at several temperatures)

Figure 1. Stress–strain curves of a carbon steel and Pb-Sb alloys (Nakamura and Kasahara (2015))

Figure 5 shows the status of the specimen at the end of the monotonic loading tests. The monotonic compression test was ended at the point when the specimen contacted to the test equipment (Fig.5 (a)). The monotonic tension test was ended because the specimen broke at the weld part of the pipe and flange (Fig.5 (b)). Figure 6 shows the load–deflection relationship of the monotonic loading. The positive displacement denotes the elbow opening direction, and the negative displacement denotes the elbow closing direction. Figure 6 expressed that the strength property was not symmetric between the opening direction and the closing direction in the elastic–plastic region. The strength of the opening direction was much higher than that of the closing direction.

Table 2 summaries the test conditions and results of the cyclic bending tests, and Fig. 7 shows the failure status of the specimens subjected to cyclic loading. The failure mode obtained by the cyclic loading tests was the fatigue failure at the elbow. However, the features of the failure were different depending on the applied displacement level. Fatigue failure occurred at the elbow flank for the specimen subjected to the ±20 mm and ±40 mm input displacement (Fig.7(a) and Fig.7(b)), whereas fatigue failure occurred at the elbow intrados for the specimen subjected to the ±65 mm input displacement (Fig.7(c)). Fatigue failure at the elbow flank is commonly observed in the experiment on the piping systems made of steel, and it is known that this failure mode is caused by the repeated elliptical deformation at the centre of the elbow.

Table 1: Material properties of Pb-Sb alloy by the tensile material test (for static loading test)

0.2% proof stress (σ_y) [MPa]	Tensile strength (σ_u) [MPa]	El. [%]
9.7	21	75.1

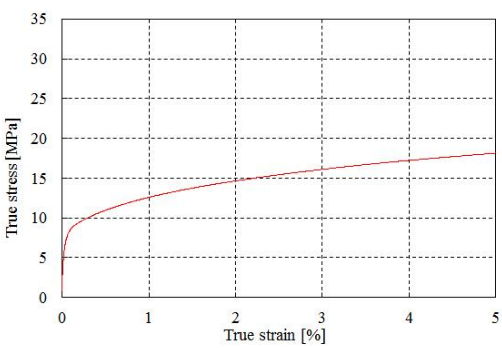

Figure 2. Stress–strain curve of Pb-Sb material

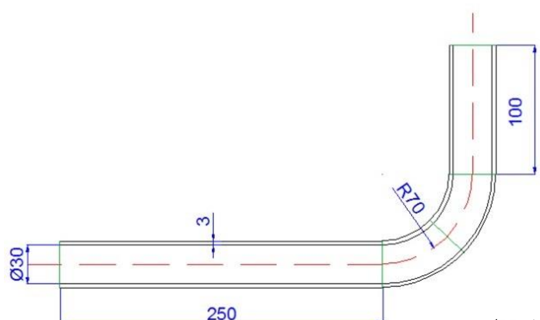

(Unit: mm)

Figure 3. Configuration of the elbow pipe

Figure 4. Setup of the static loading test

(a) Compression test

(b) Tension test

Figure 5. Status of the elbow pipe at the end of the static monotonic loading test

Fatigue failure at the intrados of the elbow came from the folding deformation at the centre of the elbow due to the excessive displacement, and the fatigue cracks from the outer surface at the elbow intrados preceded the fatigue cracks from the elbow flank. The estimated strain range at the inner surface of the flank of the elbow was approximately 2-5% for the specimens failed at the elbow flank, and approximately 10% for the specimen failed at the elbow intrados. The cyclic loading test results showed that the fatigue failure occurred on the elbow pipes made of Pb-Sb under the reversing strain condition, similar to the failure mode of elbow pipes made of steel.

Shaking table test on single-elbow pipe specimen

One-directional shaking table tests were conducted on specimens composed of an elbow made of simulation materials and an additional mass. The purpose of the shaking table tests was to observe the failure behaviour and to obtain the failure modes of a simple piping systems under excessive dynamic input.

Pb was used as the simulation material at the first step of the experimental study. However, the specimen made of Pb was too fragile and the material property was affected a lot by the air temperature or the production lots. Thus, the simulation material was changed to Pb-Sb. This paper mainly describes the results by Pb-Sb pipe specimen. Table 3 and Fig. 8 shows the material property of the simulation material.

Figure 9 shows the configuration of the test specimen. The inverted type specimen was used both in the experiment on Pb pipe specimen and Pb-Sb pipe specimen. The pendant-weight type specimen was only used in the experiment on Pb pipe specimen. The geometry of the elbow was similar to that used in the static loading test that was shown in Fig.3.

Input motions of the shaking table tests were mainly sinusoidal input that were tapered at the beginning and end of the steady amplitude portion. Figure 10 shows an example of the input sinusoidal

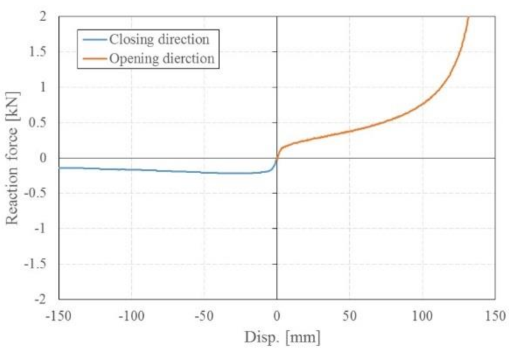

Figure 6. Load–deflection relationship of the monotonic loading test

Table 2: Summary of the static cyclic loading test

		± 20 mm	± 40 mm	± 65 mm
Measured strain [%][1]	Max	1.29	3.36	6.75
	Min	-0.45	-0.90	-2.02
Estimated strain range [%][2]		2.03	5.30	10.66
Failure mode		Fatigue	Fatigue	Fatigue
Failure position		Flank	Flank	Intrados
Num. of cycles to failure		221	66	48

[1] Strain at elbow flank, outer surface
[2] Strain at elbow flank, inner surface

(a) ±20 mm (b) ± 40 mm (c) ± 65 mm

Figure 7. Failure modes of the specimens subjected to the static cyclic load

wave. There were two cycles at the tapered potion; in the steady amplitude portion of the wave, the number of cycles was 1, 5, 10, 20, 50, or 100, depending on the purpose and the progress of the excitation test. Excitation tests were conducted by varying the additional mass, the frequency and acceleration level of the input sinusoidal wave. The static experiment to investigate the limit weight of additional mass with that the specimen be able to sustain the self-weight was also conducted on a Pb-Sb pipe specimen.

The details of the excitation tests were reported in the other papers (Nakamura and Kasahara (2016), Nakamura and Kasahara (2018)).

DISCUSSION

Failure modes by the experiments

From the experiment on Pb-Sb pipe specimens, several failure modes were obtained depending on the weight conditions and input sinusoidal wave conditions. The failure modes obtained from the excitation on the Pb-Sb single elbow specimens were as follows;

(1) Collapse by self-weight

Table 3: Material properties of simulation materials (for shaking table test)

(a) Pb-Sb

0.2% proof stress (σ_y) [MPa]	Tensile strength (σ_u) [MPa]	El. [%]
4.33	22.43	55.09

(b) Pb

0.2% proof stress (σ_y) [MPa]	Tensile strength (σ_u) [MPa]	El. [%]
5.0	10.5	87.2

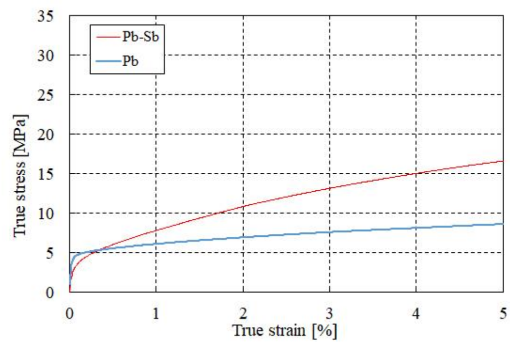

Figure 8. Stress–strain curve of Pb-Sb material for the shaking table test

(a) Inverted type specimen

(b) Pendant-weight type specimen

Figure 9. Configuration of the test specimen

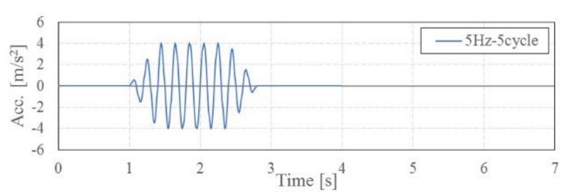

Figure 10. Example of the input sinusoidal wave (5Hz-5cycles)

(2) Collapse by a few cycles of input
(3) Ratchet and subsequent collapse
(4) No failure

The most typical failure mode was the ratchet and subsequent collapse. Figure 11 shows the typical sequence of the ratchet and subsequent collapse. The residual deformation was caused by an excitation, it accumulated as repeating excitations, and finally the specimen ended in collapse by gravity effect. "Collapse by a few cycles of input" occurred this sequence with very few input cycles. The failure mode was judged as "no failure" when the deformation of the specimen was small after 100 – 500 input cycles.

The failure behaviour of Pb pipe specimens was similar to that of the Pb-Sb pipe specimens for the inverted type specimen, that is, the typical failure mode was the ratchet and subsequent collapse. For the pendant-weight type specimen, the failure mode was;
(5) Overall deformation
Figure 12 shows this failure mode.

Failure behaviour depending on frequency ratio

The relationship between the frequency ratio and the failure modes was examined for the test results of Pb-Sb pipe specimens. It is pointed out in the previous studies that the failure modes were affected by the input acceleration level, the weight of additional mass, and the frequency ratio (Bari et al. (2017), Nakamura and Kasahara (2018)). Here, the frequency ratio was defined by the following equation;

$$f_R = \frac{f_i}{f_o} \quad (1)$$

Where f_R: the frequency ratio, f_i: the frequency of input sinusoidal wave, f_o: the natural frequency of the specimen in the elastic region.

The mass ratio M_R was used for discussing the effect of weight of additional mass. The mass ratio was defined as follows;

$$M_R = \frac{M_{Exc}}{M_L} \quad (2)$$

Where M_{Exc}: the weight of additional mass in the excitation test, M_L: the limit weight of additional mass to sustain the self-weight obtained by the self-weight collapse test in the inverted type specimen. Table 4 shows M_L, M_{Exc}, and M_R in the experiment.

(a) Initial status
(b) After the first excitation
(c) Final status (collapse)

Figure 11. Typical failure process of the inverted type specimen

Figure 12. Failure mode of the pendant-weight type specimen

Figure 13 shows the relation between the frequency ratio and the number of cycles to cause failure (N_{app}) depending on the mass ratio. The input acceleration was approximately 4 m/s^2 for all cases in Fig. 13. Open marks in these graphs denote that the specimen did not fail after the input cycles indicated in the vertical axis (their failure mode was judged as "No failure"). Solid marks denote the specimens ended in the failure mode as the ratchet and subsequent collapse. The results show that the ratchet and subsequent collapse was prone to occur when f_R was in the range of 0.7-1.0. When f_R was less than approximately 0.5, N_{app} tended to increase a little. This tendency was thought to be due to the reduction of specimen's dominant frequency in the inelastic region. The reduction ratio of natural frequency appeared to be approximately 30% from the relation between f_R and N_{app} at M_R=0.64. N_{app} increased remarkably when f_R was over 1.0. The failure was unlikely to occur when f_R was equal to 2.0, because the specimen did not respond by the input sinusoidal wave and the strain caused on the specimen was very small. Figure 13 also shows that N_{app} tended to increase as M_R decreased. It indicated that the constant primary stress caused by the dead weight was one important factor to cause failure to the specimen.

Figure 14 shows the relation between the input acceleration and N_{app} for the same f_R and M_R. It was obviously that the larger input acceleration caused the failure mode with smaller N_{app}.

Strain behaviour

Fatigue failure that has been reported as the typical failure mode of steel pipes in a lot of previous studies did not appeared in the shaking table tests on single Pb-Sb elbow pipe specimens, whereas the fatigue

Table 4. Limit weight of the additional mass and the mass ratio used in the excitation test on Pb-Sb pipe specimen

M_L	M_{Exc}	4.5kg	3.5kg	3kg	2.5kg
7.0kg	M_R	0.64	0.5	0.43	0.38

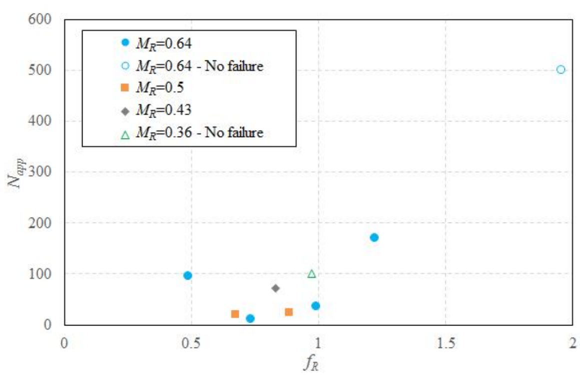

Figure 13. Relation between the frequency ratios and number of applied cycles (Input acceleration: 4m/s^2)

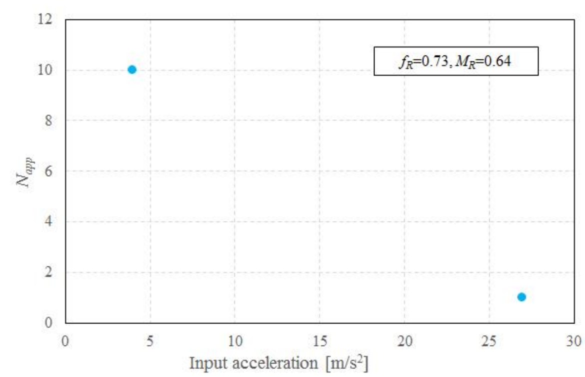

Figure 14. Relation between the input acceleration and number of applied cycles

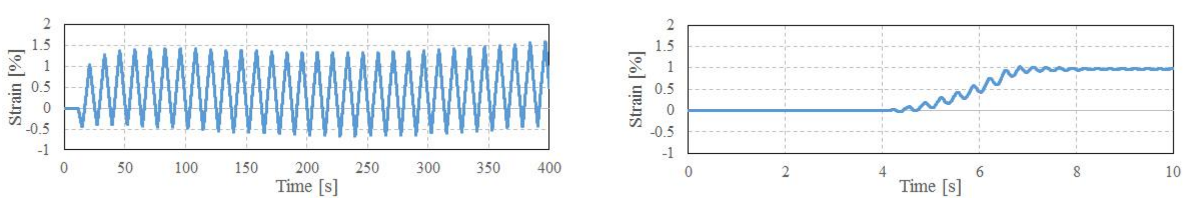

(a) Static cyclic test (±20 mm) (b) Shaking table test (f_R=0.73, M_R=0.64, 4m/s^2)

Figure 15. Strain behaviour at the flank of elbow in the static cyclic loading and shaking table test

failure occurred in the static cyclic loading test on Pb-Sb elbow pipe specimens. Figure 15 shows the examples of strain behaviour at the flank of elbow of the static loading tests and shaking table test. The strain by the static loading test showed cyclic behaviour and the mean strain was not so large. The strain range was approximately 2%. In contrast to the static loading test, the strain by the shaking table test shows large increase of the mean strain but the strain range was not so large, approximately 0.22%. The difference of the static loading test and the shaking table test appeared to be the difference of load condition; the static loading test was conducted under the displacement-control, whereas the inertial force was applied on the specimen in the shaking table test. As an elbow has the load–deflection characteristics as shown in Fig.6, the deformation by the inertial force was prone to occur to the elbow closing direction when the inertial force was applied. Thus, the ratchet behaviour rather than cyclic strain dominated the failure behaviour of the specimen in the shaking table test. Fatigue failure mode would be a failure mode when the large cyclic strain was caused in piping systems under seismic loads, from various previous studies and the static loading test on Pb-Sb pipe.

Effect of gravity

In the experiment on Pb pipe specimens, the failure mode of the inverted type specimen was the ratchet and subsequent collapse. Meanwhile, the failure mode of the pendant-weight type specimen was the overall deformation under same f_R, M_R, and input acceleration condition. The difference of these test cases was the gravity effect on the elbow deformation; gravity affected to enhance deformation for the inverted type specimen, whereas it affected to return the weight to the neutral position for the pendant-weight type specimen. Moreover, elbow's load–deformation property shown in Fig.6 was also affected to cause the failure mode. Figure 6 shows that the load–deflection curve in the elbow closing direction had the negative slope at the large plastic region, and the collapse failure was easy to occur by the load control condition like gravity. When the response behaviour remained in the elastic or slightly plastic region, the direction of the gravity effect might have not so significant. However, considering BDBE condition which would be accompanied by a large plastic deformation, the difference of the direction of gravity effect would be cause significant difference in the failure behaviour. The difference of the failure behaviour between the inverted type specimen and the pendant weight type specimen indicated that the importance to understand the structure's ultimate behaviour when considering BDBE.

In addition to the experiments on the elbow pipes made of the simulation materials, finite element analysis (FEA) has been conducted. Figure 16 shows examples of the FEA. The results showed that the failure behaviours of the pipes made by the simulation material were well reproduced by the FEA. The results of experiments and analysis appeared that the research approach using the simulation material was effective to investigate the ultimate behaviour of piping systems.

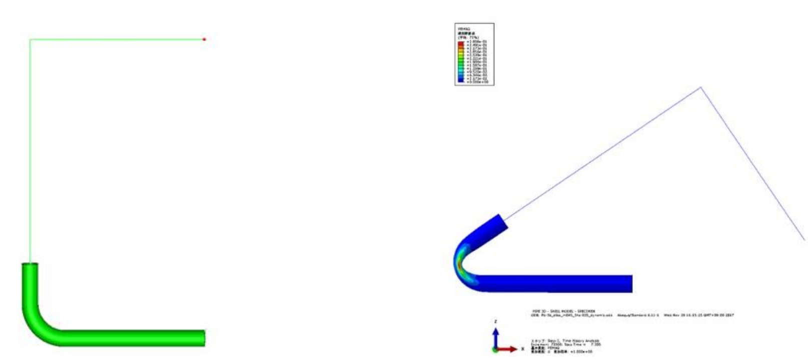

(a) FE Analysis model (b) Calculated failure mode

Figure 16. Examples of the FEA (Pb-Sb inverted type specimen)

FUTURE TASKS

Several failure modes were successfully obtained by test specimens with single elbow made of Pb-Sb alloy under dynamic cyclic load. However, the specimen's configuration was fairly simple structure in comparison with the actual piping system used in NPPs. Thus, an excitation tests on a little more complicated configuration piping system model has been conducted as the next step of this research. Figure 17 shows the configuration of the piping system model in the next stage test. Two elbow pipes made of Pb-Sb alloy were used in the piping system model. The experimental and analytical investigation are now conducted. The failure modes and the factors to cause failure for the more complicated piping system model will be reported in near future.

CONCLUSION

Experimental investigation on the failure behaviour of piping systems under the seismic events were conducted with elbow pipes made of simulation materials to clarify the possible failure modes under BDBE. The simulation materials used in the investigation were Pb and Pb-Sb alloy. The static loading test and the shaking table test on a simple piping system model were conducted, and the followings are the summary of the findings from the experiments;

(1) The failure mode from the static cyclic test was the fatigue failure. The failure modes from the shaking table test on the specimen composed of an elbow and an additional mass were " Collapse by self-weight", "Collapse by a few cycles of input", " Ratchet and subsequent collapse"," Overall deformation" and "No failure" depending on the configuration of the test specimen, the relation between the input frequency and the specimen's natural frequency, the weight of the additional mass, and the input acceleration level. The most typical failure mode was the ratchet and subsequent collapse.

(2) The failure modes were able to be classified depending on the frequency ratio and the mass ratio for the single elbow pipe specimen. Although fatigue failure was not appeared in the shaking table test, it was considered due to the specimen's configuration. Fatigue failure would occur on the pipes made of the simulation material when a large cyclic strain was caused.

(3) Considering BDBE condition which would be accompanied by a large plastic deformation, the difference of the direction of gravity effect would be cause significant difference in the failure behaviour. It is crucial to understand the structure's ultimate behaviour when treating BDBE.

(4) FE analysis was well reproduced the behaviour of the specimen made of the simulation material. The research approach using simulation materials was effective to investigate the ultimate behaviour of piping systems.

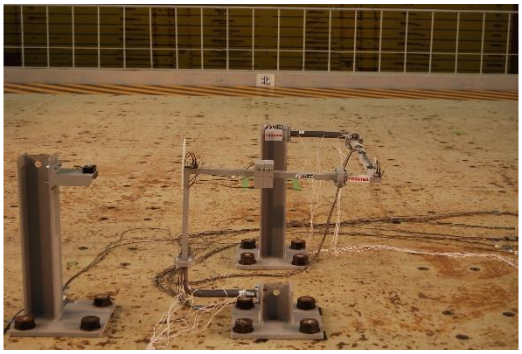

Figure 17. Configuration of the piping system model in the next stage test

ACKNOWLEDGEMENT

The research described in this paper is part of a research project named "Prevention of catastrophic boundary failure by introducing fracture control concept" (PD: Professor N. Kasahara at the University of Tokyo). The research project is sponsored by the Ministry of Education, Culture, Sports, Science and Technology of Japan (MEXT). The authors wish to extend their appreciation to MEXT for funding and supporting the research program. The authors also gratitude Mr. Y. Okuda, Mr. G. Nakamura, Mr. S. Ohkuma and Mr. T. Fukushima of Toshiba Energy Systems & Solutions Corporation for their contribution to conduct the experiments.

REFERENCES

Bari, M. A. A., Sakemi, R., and Kasahara, N. (2017) "Failure Mode Map of Pipes under Dynamic Loadings", *Proc. of the ASME PVP2017,* Hawaii, U.S., PVP2017-65635.

Fujita, K., Shiraki, K., Kitade, K., and Nakamura, T. (1978) "Vibration Damaged Experiments of Curved Piping for Investigating the Seismic Ultimate Strength", *Transactions of the JSME*, the JSME, Tokyo, Japan, 44 - 386, pp. 3437 – 3445 (in Japanese).

Kasahara, N. and Sato, T. (2017). "Difference of Strength Evaluation Approach between for DBE and for BDBE", *Pro. of the ASME PVP2017*, ASME, Hawaii, U.S., PVP2017-65478.

Nakamura, I. and Kasahara, N. (2015) "An Experimental Investigation on Failure Modes of Piping Components under Excessive Seismic Load", *Transactions of SMiRT-23,* Manchester, U.K. Division V, Paper 437.

Nakamura, I. and Kasahara, N. (2016) "Trial Model Tests with Simulation Material to Obtain Failure Modes of Pipes under Excessive Seismic Loads", *Proc. of the ASME PVP2016*, Vancouver, Canada, PVP2016-63422.

Nakamura, I. and Kasahara, N. (2016) "Improved Model Tests to Investigate the Failure Modes of Pipes under Beyond Design Basis Earthquakes", *Proc. of the ASME PVP2018*, Prague, Czech Republic, PVP2018-84424.

Nakamura, I., Otani, A., and Shiratori, M. (2010) "Comparison of Failure Modes of Piping Systems with Wall Thinning Subjected to In-Plane, Out-of-Plane, and Mixed Mode Bending Under Seismic Load: An Experimental Approach", *Transactions of the ASME, Journal of Pressure Vessel Technology*, U.S., 132, pp. 031001-1 – 031001-8.

Ravikiran, A., Dubey, P. N., Agrawal, M. K., Reddy, G. R., Singh, R. K., and Vaze, K. K. (2015) "Experimental and Numerical Studies of Ratcheting in a Pressurized Piping System Under Seismic Load", *Transactions of the ASME, Journal of Pressure Vessel Technology*, U.S., 137, pp. 031011-1-031011-7.

Tagart, S.W., Jr., Tang, Y. K.,Guzy, D. J., and Ranganath, S. (1990) "Piping dynamic reliability and code rule change recommendations", *Nuclear Engineering and Design*, Elsevier, Netherlands, 123, pp. 373-385.

Touboul, F., Blay, N., and Lacire, M. H., 1999, "Experimental, Analytical, and Regulatory Evaluation of Seismic Behavior of Piping Systems", *Transactions of the ASME, Journal of Pressure Vessel Technology*, the ASME, U.S., 121, pp. 388 – 392.

Varelis, G.E., Karamanos, S.A., and Gresnigt A.M. (2013) "Pipe Elbows Under Strong Cyclic Loading", *Transactions of the ASME, Journal of Pressure Vessel Technology*, U.S., 135, pp. 011207-1-011207-9.

Yoshino, K., Endou, R., Sakaida, T., Yokota, H., Fujiwaka, T., Asada,Y., Suzuki, K., 2000, "Study on Seismic Design of Nuclear Power Plant Piping in Japan Part 3: Component Test Results", *Proc. of the ASME PVP2000*, Seattle, U.S., 407, pp.131-137.